High-resolution magnetization studies of the heavy-fermion superconductor $CeCu_2Si_2$ at very low temperatures and in high magnetic fields

T. Tayama,* M. Lang,† T. Lühmann, and F. Steglich
Max-Planck Institute for the Chemical Physics of Solids, 01187 Dresden, Germany

W. Assmus
Institute for Physics, Frankfurt University, 60054 Frankfurt, Germany
(Received 16 December 2002; published 6 June 2003)

We report high-resolution dc-magnetization measurements on high-quality stoichiometric single crystals of $CeCu_2Si_2$ at very low temperatures down to 50 mK and in high magnetic fields up to 115 kOe, especially focusing on the as yet still unidentified phase A (and B at higher fields) that competes for stability with the heavy-fermion superconductivity. Anomalies at the A/B phase transitions are clearly observed in both the temperature and the field dependence of the magnetization. In isothermal magnetization curves $M(T=\text{const},H)$ at 50 mK, a metamagneticlike first-order transition is observed at 71 kOe and 30 kOe for $H\|a$ and c, respectively. The magnitude of the magnetization jump at the first-order transition is only $2\times10^{-3}\mu_B$/Ce and $8\times10^{-4}\mu_B$/Ce for $H\|a$ and c, respectively. Detailed magnetic phase diagrams are presented for both field orientations. The present results are consistent with a scenario that both A and B phases are spin-density-wave-type long-range-ordered states, where the ordered moments are of the order of $10^{-3}\mu_B$/Ce.

DOI: 10.1103/PhysRevB.67.214504 PACS number(s): 74.25.Dw, 74.25.Ha, 74.25.Op, 74.70.Tx

I. INTRODUCTION

Since the discovery of superconductivity in the compound $CeCu_2Si_2$ in 1979,[1] much work has been devoted to unravelling the complex properties of this archetype heavy-fermion superconductor. Early on, it was recognized that $CeCu_2Si_2$ shows an extreme sensitivity of its physical properties against variations of the sample composition. By means of a thorough thermodynamic study of the ternary chemical Ce-Cu-Si phase diagram, up to four different ground states belonging to different sectors of the homogeneity range of the primary 1:2:2 phase were found to exist.[2,3] While Cu-rich samples become superconducting (S type), small Si excess results in a still not fully identified, though most likely, magnetic phase A (A type). For larger Si excess, a related phase X (X type) has been observed.[4] We concentrate here on the fourth variant, the so-called A/S type, which exhibits a transition into phase A at T_A followed by a superconducting (sc) transition at $T_c \leqslant T_A$.

A detailed H-T phase diagram for $H\|a$ of an A/S-type sample has been reported in Ref. 7, based on elastic constant and thermal expansion measurements on a high-quality single crystal. At zero field, two closely spaced phase transitions occur; one is a sc transition at $\sim$0.68 K which, upon cooling, replaces the A phase that forms below 0.7 K.[7] For sufficiently strong magnetic fields, a high-field phase B becomes stabilized. The A/B-phase transitions have hitherto been seen in ultrasound,[7] thermal-expansion,[8,9] specific-heat,[8,10,11] muon-spin-rotation (μSR),[12] nuclear-magnetic-resonance,[13] and resistivity measurements.[14] The pronounced signatures at the A/B-phase transition observed in the thermodynamic properties, i.e., specific heat and thermal expansion,[8,10,11] indicate that the heavy quasiparticles are involved in the formation of these states. Nevertheless, there is still some uncertainty in the nature of both phases.

A comparison of the results of nuclear quadrupole resonance and μSR indicates that phase A is a dynamically magnetically ordered state characterized by slow magnetic fluctuations ($\tau\sim10^{-7}$ s).[13,12] Elastic neutron-scattering experiments have failed so far to detect any magnetic Bragg peaks in phase A. In addition, substitution studies starting from $CeCu_2Ge_2$ revealed that phase A is connected with an incommensurate antiferromagnetically ordered state.[15,16] Recently, non-Fermi-liquid (NFL) behavior has been found in the paramagnetic state near phase A by electrical resistivity, $\rho(T)$, and specific heat, $C(T)$, measurements.[14] The observation of NFL behavior in $\rho(T)$ and $C(T)$ in certain field and temperature regions, which follow the predictions for a three-dimensional antiferromagnetic quantum critical point, is consistent with the view that phase A is a spin-density-wave (SDW)-type ordered state.

Although the A and B phases are widely believed to be a SDW-like magnetically ordered state, there is no direct evidence for that until now. In this paper, we report results of high-resolution dc-magnetization measurements on high-quality stoichiometric single crystals of $CeCu_2Si_2$ at very low temperatures down to 50 mK and in high magnetic fields up to 115 kOe, applied along the a and c directions of the tetragonal $ThCr_2Si_2$ structure. Anomalies accompanied by the A/B-phase transitions are clearly observed in both the temperature and the field dependence of the magnetization. Following these anomalies as a function of temperature and field provides new details of the H-T phase diagrams. Our observations are consistent with a scenario that both the A and B phases are SDW ordered states with an extremely small-ordered moment.

The paper is organized as follows. After a description of the experiment in Sec. II, we show magnetization results in Sec. III. In Sec. IV, an analysis of the magnetization data is given, followed by a discussion on the phases A/B in Sec. V.

The paper closes with a summary in Sec. VI. A preliminary report on part of the data has been given in Ref. 17.

II. EXPERIMENT

For the present measurements, two rectangular-shaped single crystals (No. 1, 5.36 mg; No. 2, 4.84 mg), cut from the same ingot, have been used. According to x-ray diffraction measurements, the crystals are in single phase with the proper $ThCr_2Si_2$ structure. The No. 1 and 2 samples were used for measurements in fields applied along the tetragonal *a* and *c* axes, respectively. The same single crystals were previously studied by resistivity[14] and specific-heat measurements.[10,11] The residual resistivities are 10 $\mu\Omega$ cm and 5.9 $\mu\Omega$ cm for crystal Nos. 1 and 2, respectively.[14] To perform dc-magnetization measurements at very low temperatures down to 50 mK and in high magnetic fields up to 115 kOe, we developed a Faraday-force capacitive magnetometer with an extremely high resolution, enabling the detection of magnetic moments smaller than 10^{-6} emu. As for details of this technique, we refer to Ref. 18. In all measurements, a field gradient of 1 kOe/cm was applied in addition to the homogeneous external magnetic field. In the field-scan measurements, small field-sweep rates of 100 Oe/min (500 Oe/min) were used below (above) 15 kOe to maintain a constant sample temperature. A commercial superconducting quantum interference device magnetometer (MPMS, Quantum Design Co.) was utilized in the temperature range from 2 K to 400 K.

III. RESULTS

Figure 1 shows the temperature dependence of the dc susceptibility $\chi(T)$ defined as $M(T)/H$ of $CeCu_2Si_2$ at a fixed magnetic field of 5 kOe applied along the *a* and *c* axes. After zero-field cooling (ZFC) the sample to a temperature ≈ 1 K, i.e., well above the transition temperatures of interest, the data at lower temperatures were obtained by slowly warming up from the base temperature of 0.05 K to 1 K in zero field (ZFC) and by subsequently cooling down in a finite field (FC).

Upon cooling starting from room temperature, the $\chi(T)$ curves increase with a distinct magnetic anisotropy. The susceptibility for the *c* axis, χ_c, is larger than that for the *a* axis, χ_a. The inset of Fig. 1 displays the inverse susceptibilities $1/\chi(T)$ which roughly follow a Curie-Weiss law for temperatures down to ~ 150 K. The average susceptibility $\chi_{av}(T) \equiv [2\chi_a(T)+\chi_c(T)]/3$ allows us to estimate an effective magnetic moment μ_{eff} and the Weiss constant θ by using a fit of the form $\chi(T)=N_A\mu_{eff}^2/3k_B(T-\theta)$, where N_A is the Avogadro number and k_B the Boltzmann constant. The estimated values of μ_{eff} and θ are $2.48\mu_B$ and -76 K, respectively. These values are in good agreement with those determined in previous studies.[24,25] For temperatures below about 80 K where χ exhibits a change of slope, the *T* dependence of the χ curves gradually becomes smaller merging into an almost *T*-independent behavior below about 10 K. This reflects the crossover from a paramagnetic high-temperature state to a seemingly nonmagnetic low-temperature state.

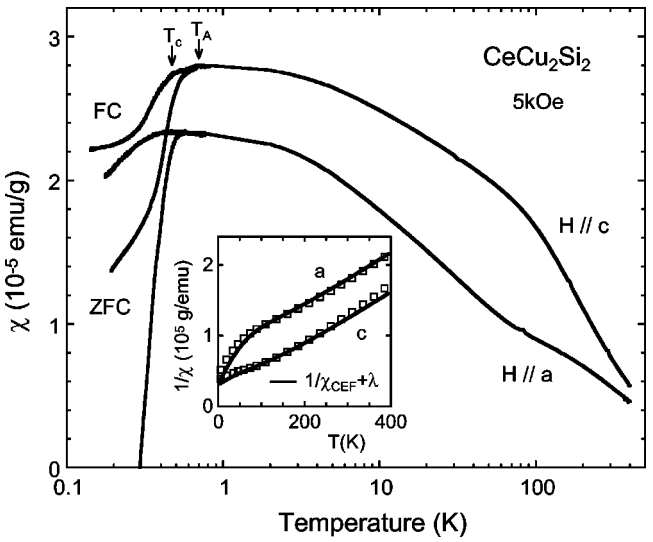

FIG. 1. Temperature dependence of the dc susceptibility $\chi(T)$ defined by $M(T)/H$ of $CeCu_2Si_2$ for the *a* and *c* directions at a fixed field of 5 kOe, plotted on a logarithmic temperature scale. FC and ZFC denote field cooling and zero-field cooling, respectively. T_c and T_A are the transition temperatures into the superconducting state and phase *A*, respectively. The inset shows the inverse of the susceptibilities at 5 kOe. Solid lines denote model curves that take into account the crystal-field interaction in addition to a mean-field exchange interaction coefficient λ of -5×10^4 g/emu.

At ~ 0.6 K, the sc transition occurs, which manifests itself in the opening of a large hysteresis between the FC and ZFC $\chi(T)$ data. The FC $\chi(T)$ curve shows a sharp kink at about 0.45 K followed by a rapid reduction. This indicates that a bulk sc transition occurs at this temperature. Here, we define the sc transition temperature T_c as the kink position in the FC $\chi(T)$ curve. It should be noted that the hysteresis already opens above the so-derived T_c value, demonstrating that a small fraction of the sample has a higher T_c. In addition to the sc transition, the $\chi(T)$ curve shows a rather small but distinct kink at the *A*-phase-transition temperature T_A of 0.7 K, as determined by the elastic constant and thermal expansion measurements.[7,9]

To display the anomaly at T_A more clearly, the low-*T* data for $T \leqslant 0.8$ K are shown in Figs. 2 and 3 for several fields applied along the *a* and *c* axes, respectively. The sc state becomes rapidly suppressed by the field and only the *A*-phase transition remains visible at 20 kOe. The inset of Fig. 2 shows the magnetization at 20 kOe normalized to its value at T_A, $M(T)/M(T=T_A)$. The $M(T)$ curve for $H\|a$ is only weakly temperature dependent below T_A, whereas the $M(T)$ curve for $H\|c$ decreases significantly upon cooling below T_A. Surprisingly, the reductions seen in the magnetization below T_A amount to only 1% and 5% for $H\|a$ and c, respectively. This result indicates that the ordered magnetic moment in phase *A* is extremely small. As the field increases, T_A shifts towards lower temperatures. For $H\|a$, the data at 60 kOe still show a clear signature of the *A*-phase transition at about 0.5 K [Fig. 2(b)], where the $M(T)$ curve bends downwards. In contrast, the data taken at 80 kOe reveal a sudden increase at almost the same temperature of 0.5 K.

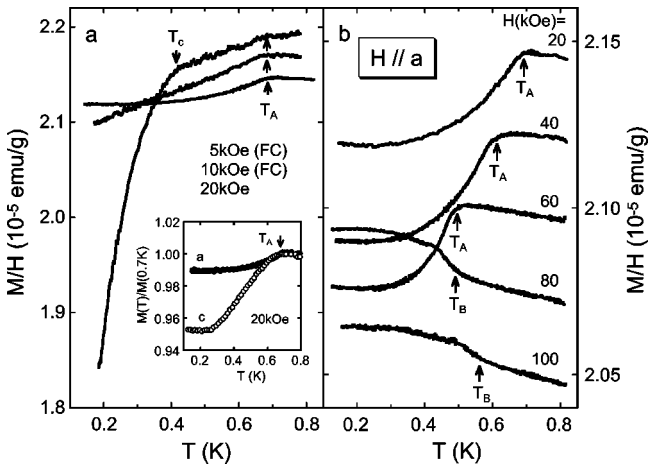

FIG. 2. Temperature dependence of the magnetization as M/H for $H\|a$ at various fields. Arrows indicate the transition temperatures into phases A and B, T_A and T_B, respectively. FC was employed for the data at 5 and 10 kOe, while all other data were taken after ZFC. The inset in Fig. 2 shows the T dependence of magnetization normalized to its value at T_A.

Furthermore, this anomaly is found to shift to a higher temperature with increasing fields.[26] Assigning the latter feature to the transition into phase B yields a H-T phase diagram, consistent with that derived from the elastic constant and the thermal expansion measurements,[7] which revealed the appearance of phase B in fields in excess of 70 kOe for $H\|a$. Therefore, the upward-bent anomaly in the M/H curve is attributed to the B-phase transition. As shown in Fig. 3(b), a similar upward-bent anomaly is also seen for $H\|c$ in fields above 40 kOe, where the transition temperature is also found to increase with the field. These observations demonstrate that phase B exists also for $H\|c$.

Figure 4 shows isothermal magnetization curves $M(H)$ taken at the base temperature of 50 mK for fields up to 115 kOe applied along the a and c axes. The data collected with

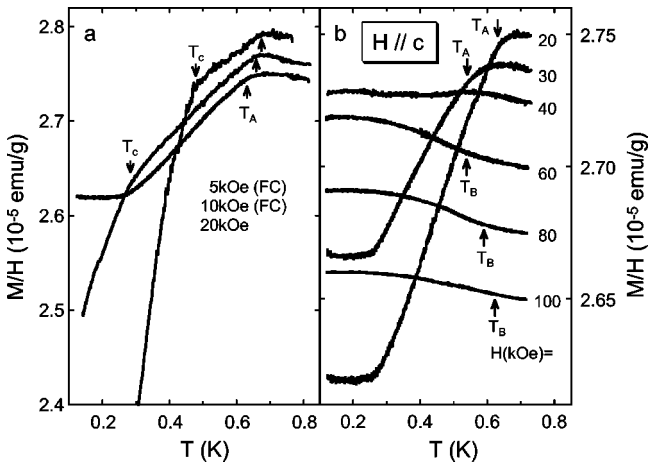

FIG. 3. Temperature dependence of the magnetization as M/H for $H\|c$ at various fields. Arrows indicate the transition temperatures into phases A and B, T_A and T_B, respectively. FC was employed for the data at 5 and 10 kOe, while all other data were taken after ZFC.

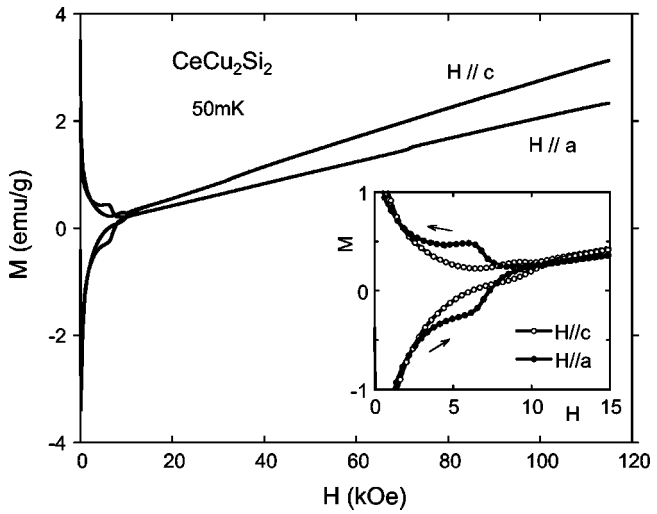

FIG. 4. Isothermal magnetization $M(H)$ curves of $CeCu_2Si_2$ for $H\|a$ and c at the base temperature of 50 mK. The data were obtained after zero-field cooling the sample from a temperature well above T_c. Inset shows the enlarged low-field part below 15 kOe.

the increasing and, subsequently, the decreasing fields were obtained after zero-field cooling the sample from a temperature well above T_c. A strong irreversibility associated with the sc state is clearly seen in fields below about 15 kOe, cf. the inset of Fig. 4. For $H\|c$, the irreversibility becomes continuously smaller as the field approaches the upper critical field H_{c2}. On the contrary, the irreversibility in the $M(H)$ curve for $H\|a$ does not change significantly in the intermediate field range from 3 to about 6 kOe and decreases suddenly near H_{c2}. Such an anomaly slightly below H_{c2} is often called the ''peak effect.'' Apparently in the present case, the peak effect is considerably stronger for $H\|a$ than that for $H\|c$.

The isothermal magnetization curves taken at several temperatures below T_c are shown in Fig. 5. At 430 mK, i.e., near

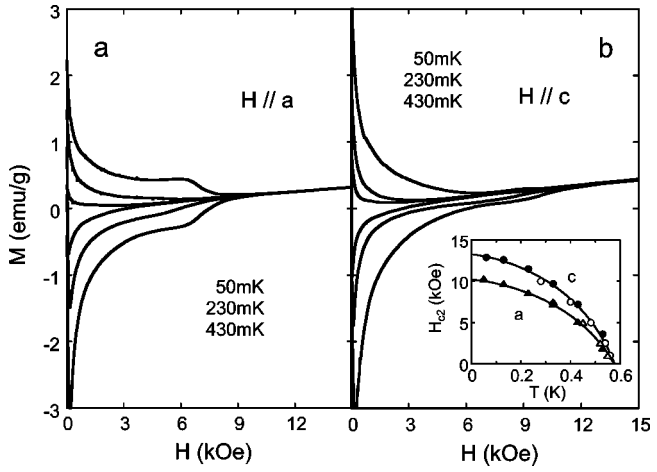

FIG. 5. Isothermal magnetization $M(H)$ curves of $CeCu_2Si_2$ with $H\|a$ (a) and $H\|c$ (b) at various temperatures below $T_c(B=0)$. The inset shows the temperature dependence of the upper critical field H_{c2}. The experimental procedure employed to determine H_{c2} is given in the text.

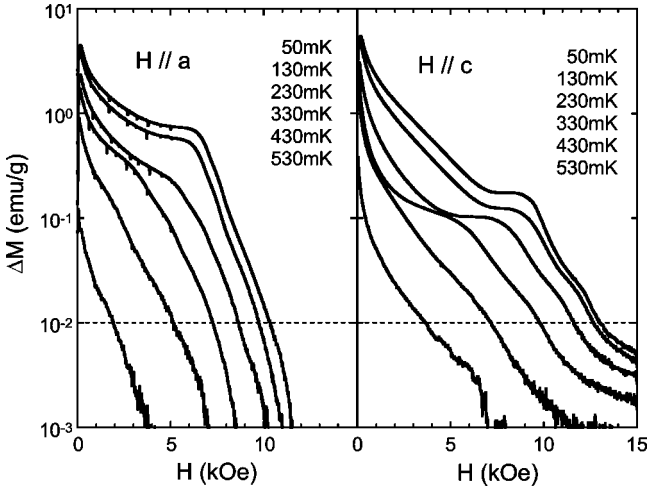

FIG. 6. Difference in the magnetization taken upon increasing and decreasing the field as a function of the field for the *a* and *c* directions at various temperatures.

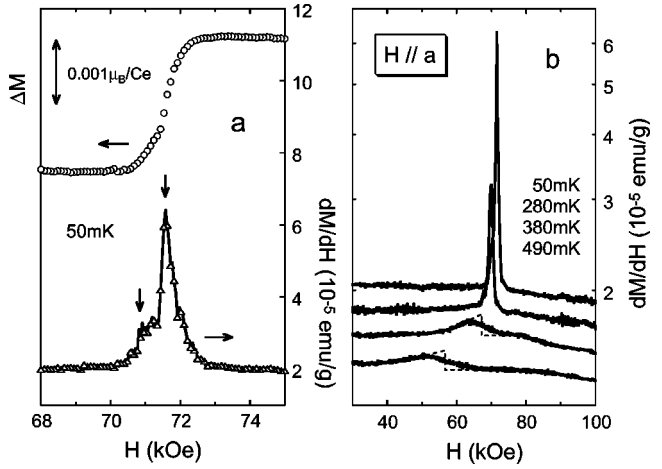

FIG. 7. Field dependence of (a) the isothermal magnetization ΔM after subtracting an appropriate linear contribution (left scale) as well as the differential susceptibility dM/dH (right scale) for $H\|a$ at 50 mK. (b) The dM/dH curves at various temperatures. The broken lines correspond to midpoint constructions as described in the text.

T_c at $B=0$, the data for both field orientations are quite similar. In contrast, the data taken at temperatures far below T_c reveal a clear difference between both field orientations. The width of the hysteresis between the increasing- and decreasing-field curve, $\Delta M = M_{\text{increase}} - M_{\text{decrease}}$, which is proportional to a critical-current density in the sc state, is shown in Fig. 6 on a semilogarithmic scale. In the dc-magnetization measurement, H_{c2} can be defined by the field where the critical current becomes zero, i.e., $\Delta M = 0$. In the present case, however, a small but finite critical current can still be discerned even in relatively high fields, especially for $H\|c$. This observation also demonstrates that a small fraction of the sample volume has a higher T_c. Accordingly, we define H_{c2} as the field where ΔM reaches a certain value, here chosen as 10^{-2} emu/g. Using this criterion provides $T_c(H)$ values consistent with those obtained from the $M(T)$ data. The so-derived phase diagram for the sc state is shown in the inset of Fig. 5. The anisotropy ratio for H_{c2}, i.e., H_{c2}^c/H_{c2}^a, amounts to about 1.25 in accordance with the previous results.[19,20]

Now we turn our attention to the *A* and *B* phases. As shown in Fig. 4, the $M(H)$ curves at 50 mK for both field orientations are nearly straight lines in fields above H_{c2} up to 115 kOe, the maximum field available except for small step-like anomalies for both field directions. This becomes clearer in Figs. 7 and 8, where we show differential susceptibilities dM/dH for $H\|a$ and *c*, respectively. For $H\|a$, an extremely sharp peak appears at 71 kOe in the dM/dH curve at 50 mK, indicating that a first-order transition from phase *A* to phase *B* occurs at this field value. This transition field coincides with that determined by the elastic constant and magnetostriction experiments.[7,9] The magnetization curve after subtracting an appropriate linear contribution is also shown in the figure as $\Delta M(H)$. Remarkably, the magnitude of the magnetization jump at 71 kOe corresponds to a change of the magnetic moment of only $0.002\mu_B$/Ce for $H\|a$, consistent with what has been found by the field modulation technique.[21] Upon warming, the sharp peak found at 50 mK drastically becomes smaller and shifts to lower fields, as shown in Fig. 7(b). In the dM/dH data above 380 mK, only one second-order transition is seen at 65 kOe. Since the transition is rather broad, we define the transition field by a midpoint construction, as denoted by the broken line. Similarly, the dM/dH curves at 50 mK for $H\|c$ also indicate two transitions: a first-order transition at 31 kOe and a second-order transition at 42 kOe. As shown in Fig. 8(a), the magnitude of the magnetization jump at 31 kOe is less than $0.001\mu_B$/Ce. Regarding the broad second-order transition at 42 kOe, the transition field is defined by a midpoint construction, similar to that used for $H\|a$. These observations are consistent with results of magnetoresistance measurements for the same sample,[23] which also indicate two anomalies at 32 kOe and

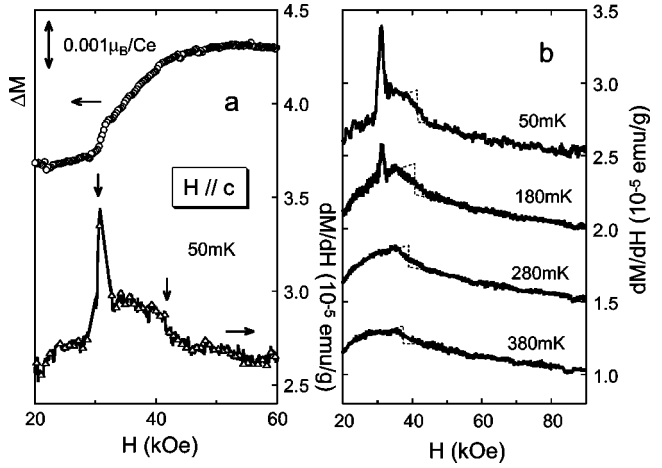

FIG. 8. Field dependence of (a) the isothermal magnetization ΔM after subtracting an appropriate linear contribution (left scale) as well as the differential susceptibility dM/dH (right scale) for $H\|c$ at 50 mK. (b) The dM/dH curves at various temperatures. The broken lines correspond to midpoint constructions as described in the text.

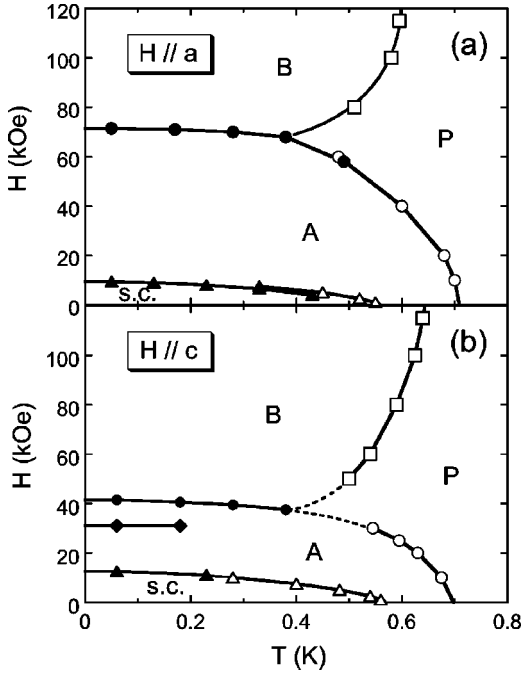

FIG. 9. Magnetic phase diagrams for $H\|a$ (a) and $H\|c$ (b). *A*, *B*, and *P* denote phase *A*, phase *B*, and the paramagnetic phase, respectively. The open and close symbols represent the position of the phase transition determined from the temperature and the field dependence of the magnetization, respectively.

45 kOe in the $\rho(H)$ curve at 20 mK.

The *H*-*T* phase diagrams constructed by the present measurements are shown in Fig. 9. *P*, *A*, and *B* represent the paramagnetic phase, the *A* phase, and the *B* phase, respectively. The phase diagram for $H\|a$ is in good agreement with the previous result,[7] while that for $H\|c$ is presented for the first time, to the best of our knowledge. The sc phase is situated in the low-field region and is surrounded by phase *A*. The latter is found to be more stable for $H\|a$ than for $H\|c$. T_A decreases as the field increases, while T_B increases with H up to 115 kOe for both field orientations.

At the end of this section, we show results for the de Haas–van Alphen (dHvA) effect obtained from the present magnetization measurements. In order to illustrate clearly the dHvA effect, we show in Fig. 10 the field derivatives of the raw data, being proportional to the sample magnetization, at 50 mK for both field directions as a function of the inverse field. A periodic oscillation is clearly seen for both directions. Since, in addition, a characteristic T dependence for the oscillations is found, the oscillation can be ascribed to the dHvA effect.

IV. ANALYSIS

A. The crystalline electric-field interaction

Here, we analyze the magnetic susceptibility given in Fig. 1 by taking into account the crystalline electric-field (CEF) effect. The CEF interaction separates the sixfold degenerate ground-state multiplet $^2F_{5/2}$ of the trivalent Ce ion into three doublets: Γ_{t6}, $\Gamma_{t7}^{(1)}$, and $\Gamma_{t7}^{(2)}$. The energy levels for the three

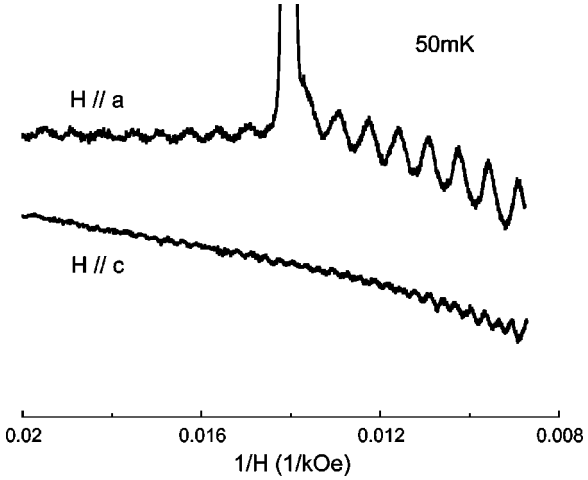

FIG. 10. The de Haas–van Alphen oscillations for $H\|a$ and *c* at 50 mK as a function of the inverse field. The ordinate is the field differential of the capacitance which is proportional to the sample magnetization. An anomaly at 0.014/kOe for $H\|a$ is ascribed to the first-order transition from phase *A* to *B*.

doublets have been determined via inelastic neutron-scattering experiments on $CeCu_2Si_2$,[24] cf. Table I.

The ground state is the Kramers doublet $\Gamma_{t7}^{(1)}$. The two excited doublets are degenerate and separated from the ground state by 340 K. By using these energy levels, we fit the measured magnetic susceptibility by the following form $1/\chi = 1/\chi_{CEF} - \lambda$, where χ_{CEF} is the CEF susceptibility and λ is the molecular-field constant. The best fit is obtained for $\lambda = -5 \times 10^4$ g/emu, cf. solid lines in the inset of Fig. 1. The calculations are in good agreement with the experimental results for temperatures above 100 K, meaning that the above CEF level scheme also applies to the A/S-type samples. The obtained λ is three times larger than that found in Ref. 24 for reasons that are unknown at present. Horn *et al.* and Holland-Moritz *et al.* have also reported a CEF level scheme.[28,29] However, calculations based on their level scheme do not provide a proper fit to the experimental data. The same observation was made also by Goremychkin *et al.* As a result, the present data support the CEF level scheme proposed by Goremychkin *et al.*, where the first excited state lies 340 K above the ground state. Therefore, at sufficiently low temperatures we can ignore any contributions from the excited states, and the properties should reflect the character of the $\Gamma_{t7}^{(1)}$ Kramers doublet.

B. The de Haas–van Alphen oscillations

In this section, we analyze the dHvA oscillations displayed in Fig. 10. The dHvA effect provides useful informa-

TABLE I. Energy levels and wave functions taken from Ref. 24.

Energy (K)	Label	Wave function
340	Γ_{t6}	$\|\pm 1/2\rangle$
340	$\Gamma_{t7}^{(2)}$	$0.47\|\mp 5/2\rangle + 0.88\|\pm 3/2\rangle$
0	$\Gamma_{t7}^{(1)}$	$0.88\|\pm 5/2\rangle - 0.47\|\mp 3/2\rangle$

TABLE II. Various physical quantities for the de Haas–van Alphen effect.

Orientation	H(kOe)	F(T)	T_D(K)	$m_i^*(m_e)$
$H\|a$	50–70	150	0.3	5
	75–110	150	0.3	5.6
$H\|c$	65–110	330	0.4	5.6

tion on the Fermi-surface parameters. The so-derived quantities are summarized in Table II. The fast Fourier-transform (FFT) analysis allows us to estimate the dHvA frequencies that correspond to extremal cross sections of the Fermi surface. The FFT analyses are done with respect to the magnetic induction B, which is expressed as $H+4\pi(1-D)M$, where D is the demagnetizing factor and M is the volume magnetization. For both field orientations, we used $D=0.6$. In the present case, only one frequency is found for both field orientations, i.e., 150 T and 330 T for $H\|a$ and c, respectively. No significant change is found for F across the first-order A-B phase transition for $H\|a$. The above results are in reasonable agreement with that obtained in the field modulation technique by Hunt *et al.*[21] and magnetoacoustic quantum oscillations by Wolf *et al.*[22] According to the Lifshitz-Kosevich formula,[30] the temperature and the field dependence of the amplitude A_i of the dHvA frequency for the extremal orbit i is given by the following expressions:

$$M_{\rm osc} \equiv A_i \sin\left(\frac{2\pi F}{B}+\phi\right), \tag{1}$$

$$A_i \propto TB^{-1/2}\frac{\exp(-\alpha m_i^* T/B)}{1-\exp(-2\alpha m_i^* T/B)}, \tag{2}$$

where $\alpha=2\pi^2 c k_B/e\hbar$. m_i^* is the cyclotron effective mass of the conduction electron averaged over the extremal orbit i and normalized by the free-electron mass m_e. The mass m_i^* is determined from the slope of the data when plotted as $\ln(A_i[1-\exp(-2\alpha m_i^* T/B)]/T)$ vs T at constant B using a method of successive approximations. The Dingle temperature T_D, which is a measure of the scattering rate by impurities, is determined from the slope of the curve in a plot $\ln[A_i B^{1/2}\sinh(\alpha m_i^* T/B)]$ vs $1/B$ at constant T. The cyclotron mass in both phases has almost the same value as that found by Hunt *et al.*[21] The obtained T_D is remarkably small, indicating that the quality of our samples is quite good. This is an important observation for investigating the A and B phases.

For $H\|a$, the dHvA amplitude in phase A is extremely reduced compared to that in phase B. In the usual magnetic materials, a reduction in the dHvA amplitude is due to a change in either the cyclotron mass (e.g., UPt_3, Ref. 31) or the Dingle temperature (e.g., $NbIn_3$, Refs. 32 and 33). In the present case, however, the origin of the amplitude reduction in phase A is not clear yet, because the cyclotron mass and the Dingle temperature are nearly the same in both phases.

V. DISCUSSION

First, we discuss the field dependence of T_A and T_B by making use of an equation that is similar to the Ehrenfest relation:

$$\Delta\left(\frac{C}{T}\right)\bigg|_{T=T_c} = -\frac{dH_c}{dT}\Delta\left(\frac{\partial M}{\partial T}\right)_H\bigg|_{T=T_c}. \tag{3}$$

Δ is defined by $\Delta Q \equiv Q_L - Q_H$, where Q_L and Q_H are physical quantities ($=C$ or M) at low-T and high-T side across a second-order phase boundary, respectively. Since $\Delta(C/T)$ is always positive, the signs of $\Delta(\partial M/\partial T)$ and dH_c/dT should be different. The present data are consistent with relation (4). For instance, $\Delta(\partial M/\partial T)_H|<0$ (Fig. 2) and $dH_c/dT>0$ [Fig. 9(a)] are established at $T_B(H=80$ kOe) for $H\|a$. Therefore, it is likely that the phases A and B are thermal equilibrium states. This observation is of relevance because the phase A/B has been frequently assigned to a quasistatic spin-glass–like, i.e., metastable state.[35,34]

Next, we discuss the first-order A-B phase boundary in the phase diagram for $H\|a$ (Fig. 7) by making use of the Clausius-Clapeyron relation

$$\Delta S = -\frac{dH_c}{dT}\Delta M, \tag{4}$$

where ΔS and ΔM denote the discontinuity of the entropy and the magnetic moment across the transition, respectively. The observed ΔM value at 50 mK is $\approx 0.002\mu_B$/Ce ($=11$ emu/mole). Assuming that the curve of $H_c(T)$ follows a form $H_0(1-(T/T_c)^2)$, the value of H_0 is estimated to be about -2×10^4 [Oe/K^2]. By substituting these values into Eq. (5), $\Delta C/T$ is found to be about 50 mJ/mole K^2. This value is close enough to the value of 70 mJ/mole K^2 obtained from the specific-heat measurements taken at 120 mK.[10,11] Accordingly, the change in the entropy at the first-order A-B phase transition mainly comes from the change in the magnetic moments. This observation supports the magnetic origin of phase A/B, consistent with the notion of phase A and B being SDW ordered states.

Very recently, Stockert *et al.* have reported results from elastic neutron-scattering measurements on single-crystalline $CeCu_2(Si_{1-x}Ge_x)_2$ for intermediate $x=0.5$ and weak doping level $x=0.05$.[36] According to their results, there is almost no change in the ordering wave vector $\tau=(0.25,0.25,0.5)$ for both crystals, but a drastic reduction occurs in the ordered moment from about $0.5\mu_B$ at $x=0.5$ to about $0.1\mu_B$ for $x=0.05$. This fits appropriately to the present results of an even more strongly reduced moment for the pure system. They also reported that the observed nesting vector τ agrees well with the nesting vector derived from the renormalized-band-structure calculations by Zwicknagl *et al.*,[37] supporting the view that phase A is a SDW ordered state.

VI. SUMMARY

We have performed high-resolution dc-magnetization measurements on high-quality stoichiometric single crystals

of $CeCu_2Si_2$ at very low temperatures down to 50 mK and in high magnetic fields up to 115 kOe, especially focusing on the *A* and *B* phases. Signatures of the *A*/*B*-phase transitions are clearly observed in both the temperature and the field dependence of the magnetization. The $M(T,H=\text{const})$ curve shows a kink at the *A*-phase-transition temperature T_A, which decreases with increasing the field. Conversely, the $M(T,H=\text{const})$ curve for both *a* and *c* directions shows an upward-bent anomaly at the *B*-phase-transition temperature T_B, which increases with the field. In isothermal magnetization curves $M(T=\text{const},H)$ at 50 mK, a metamagneticlike first-order transition is observed at 71 kOe and 30 kOe for $H\|a$ and c, respectively. Surprisingly, the magnitude of the magnetization jump at the first-order transition is only $2\times10^{-3}\mu_B$/Ce and $8\times10^{-4}\mu_B$/Ce for $H\|a$ and *c*, respectively. Furthermore, de Haas–van Alphen oscillations are clearly observed in the $M(T=\text{const},H)$ data for both field orientations. Detailed magnetic phase diagrams are constructed for both directions. The phase diagrams for $H\|c$ are presented for the first time, to the best of our knowledge. Our results are consistent with a scenario that both *A* and *B* phases are spin-density-wave long-range-ordered states, where the ordered moments are of the order of $10^{-3}\mu_B$/Ce. This result is consistent with previous neutron-diffraction experiments, which have failed to detect any magnetic Bragg peak so far.

ACKNOWLEDGMENTS

We are grateful to Philipp Gegenwart, Christoph Geibel, and Christoph Langhammer for valuable discussions.

*Present address: Institute for Solid State Physics, University of Tokyo, Kashiwa, Chiba 277-8581, Japan.

†Present address: Institute for Physics, Frankfurt University, 60054 Frankfurt, Germany.

[1] F. Steglich, J. Aarts, C.D. Bredl, W. Lieke, D. Meschede, W. Franz, and H. Schäfer, Phys. Rev. Lett. **43**, 1892 (1979).

[2] R. Modler, M. Lang, C. Geibel, C. Schank, R. Müller-Reisener, P. Hellmann, A. Link, G. Sparn, W. Assmus, and F. Steglich, Physica B **206&207**, 586 (1995).

[3] F. Steglich, P. Gegenwart, C. Geibel, R. Helfrich, P. Hellmann, M. Lang, A. Link, R. Modler, G. Sparn, N. Büttgen, and A. Loidl, Physica B **223&224**, 1 (1996).

[4] In certain $CeCu_2Si_2$ samples even ferromagnetic interactions have been observed by Ishikawa, *et al.* (Refs. 5 and 6).

[5] M. Ishikawa, N. Takeda, P. Ahmet, Y. Karaki, and H. Ishimoto, J. Phys.: Condens. Matter **13**, L25 (2001).

[6] M. Ishikawa, N. Takeda, P. Ahmet, Y. Karaki, H. Ishimoto, D. Huo, and J. Sakurai, J. Phys. Chem. Solids **63**, 1165 (2002).

[7] G. Bruls, B. Wolf, D. Finsterbusch, P. Thalmeier, I. Kouroudis, W. Sun, W. Assmus, B. Lüthi, M. Lang, K. Gloos, F. Steglich, and R. Modler, Phys. Rev. Lett. **72**, 1754 (1994).

[8] M. Lang, R. Modler, U. Ahlheim, R. Helfrich, P.H.P. Reinders, F. Steglich, W. Assmus, W. Sun, G. Bruls, D. Weber, and B. Lüthi, Phys. Scr., T **T39**, 135 (1991).

[9] M. Lang, P. Gegenwart, R. Helfrich, M. Köppen, F. Kromer, C. Langhammer, C. Geibel, F. Steglich, J. S. Kim, and G. R. Stewart, in *Electron Correlations and Materials Properties*, edited by Gonis *et al.* (Kluwer Academic, Dordrecht, MA/Plenum, New York, 1999), p. 153.

[10] C. Langhammer, Dissertation, TU Dresden, 2000.

[11] F. Steglich, P. Gegenwart, C. Geibel, P. Hinze, M. Lang, C. Langhammer, G. Sparn, T. Tayama, O. Trovarelli, N. Sato, T. Dahm, and G. Varelogiannis in *More is Different—Fifty Years of Condensed Matter Physics*, edited by N. Phuan Ong and Ravin N. Bhatt (Princeton University Press, Princeton, NJ, 2001), pp. 191–210.

[12] R. Feyerherm, A. Amato, C. Geibel, F.N. Gygax, P. Hellmann, R.H. Heffner, D.E. MacLaughlin, R. Müller-Reisener, G.J. Nieuwenhuys, A. Schenk, and F. Steglich, Phys. Rev. B **56**, 699 (1997).

[13] K. Ishida, Y. Kawasaki, K. Tabuchi, K. Kashima, Y. Kitaoka, K. Asayama, C. Geibel, and F. Steglich, Phys. Rev. Lett. **82**, 5353 (1999).

[14] P. Gegenwart, C. Langhammer, C. Geibel, R. Helfrich, M. Lang, G. Sparn, F. Steglich, R. Horn, L. Donnevert, A. Link, and W. Assmus, Phys. Rev. Lett. **81**, 1501 (1998).

[15] O. Trovarelli, M. Weiden, R. Müller-Reisener, M. Gómez-Berisso, P. Gegenwart, M. Deppe, C. Geibel, J.G. Sereni, and F. Steglich, Phys. Rev. B **56**, 678 (1997).

[16] G. Knebel, C. Eggert, D. Engelmann, R. Viana, A. Krimmel, M. Dressel, and A. Loidl, Phys. Rev. B **53**, 11 586 (1996).

[17] F. Steglich, N. Sato, T. Tayama, T. Lühmann, C. Langhammer, P. Gegenwart, P. Hinze, C. Geibel, M. Lang, G. Sparn, and W. Assmus, Physica C **341–348**, 691 (2000).

[18] T. Sakakibara, H. Mitamura, T. Tayama, and H. Amitsuka, Jpn. J. Appl. Phys. **33**, 5067 (1994).

[19] W. Assmus, M. Herrmann, U. Rauchschwalbe, S. Riegel, W. Lieke, H. Spille, S. Horn, G. Weber, F. Steglich, and G. Cordier, Phys. Rev. Lett. **52**, 469 (1984).

[20] Y. Onuki, T. Hirai, T. Komatsubara, S. Takayanagi, A. Sumiyama, A. Furukawa, Y. Oda, and H. Nagano, J. Magn. Magn. Mater. **52**, 338 (1985).

[21] M. Hunt, P. Meeson, P-A. Probst, P. Reinders, M. Springford, W. Assmus, and W. Sun, J. Phys.: Condens. Matter **2**, 6859 (1990).

[22] B. Wolf, G. Bruls, D. Finsterbusch, I. Kouroudis, and B. Luethi, Physica B **211**, 233 (1995).

[23] P. Gegenwart, Ph.D. Dissertation, TU Darmstadt, 1997.

[24] E.A. Goremychkin, and R. Osborn, Phys. Rev. B **47**, 14 280 (1993).

[25] B. Batlogg, J.P. Rameika, A.S. Cooper, G.R. Stewart, Z. Fisk, and J.O. Willis, J. Magn. Magn. Mater. **47&48**, 42 (1985).

[26] A similar field dependence was observed for the peak in the ratio of specific heat to temperature, C/T, of stoichiometric $CeCu_2Si_2$, cf. Fig. 3 in Ref. 27.

[27] B. Andraka, G.R. Stewart, and F. Steglich, Phys. Rev. B **48**, 3939 (1993).

[28] S. Horn, E. Holland-Moritz, M. Loewenhaupt, F. Steglich, H. Scheuer, A. Benoit, and J. Flouquet, Phys. Rev. B **23**, 3171 (1981).

[29] E. Holland-Moritz, W. Weber, A. Severing, E. Zirngiebl, H.

Spille, W. Baus, S. Horn, A.P. Murani, and J.L. Ragazzoni, Phys. Rev. B **39**, 6409 (1989).
[30] D. Shoenberg, *Magnetic Oscillations in Metals* (Cambridge University Press, Cambridge, 1984).
[31] K. Sugiyama, M. Nakashima, D. Aoki, K. Kindo, N. Kimura, H. Aoki, T. Komatsubara, S. Uji, Y. Haga, E. Yamamoto, H. Harima, and Y. Onuki, Phys. Rev. B **60**, 9248 (1999).
[32] I. Umehara, T. Ebihara, N. Nagai, K. Satoh, Y. Fujimaki, and Y. Onuki, J. Phys. Soc. Jpn. **61**, 1633 (1992).
[33] R. Settai, T. Ebihara, H. Sugiyama, N. Kimura, M. Takashima, H. Ikezawa, K. Ichihashi, and Y. Onuki, Physica B **201**, 102 (1994).
[34] A. Koda, W. Higemoto, R. Kadono, K. Ishida, Y. Kitaoka, C. Geibel, and F. Steglich, Physica B **281&282**, 16 (2000).
[35] Y.J. Uemura, W.J. Kossler, X.H. Yu, H.E. Schone, J.R. Kempton, C.E. Stronach, S. Barth, F.N. Gygax, B. Hitti, A. Schenck, C. Baines, W.F. Lankford, Y. Onuki, and T. Komatsubara, Phys. Rev. B **39**, 4726 (1989).
[36] O. Stockert, M. Deppe, C. Geibel, F. Steglich, D. Hohlwein, and R. Schneider, Acta Phys. Pol. B **34**, 963 (2003).
[37] G. Zwicknagl (unpublished).